Nuclear Mathematical and Computational Sciences: A Century in Review, A Century Anew
Gatlinburg, Tennessee, April 6-11, 2003, on CD-ROM, American Nuclear Society, LaGrange Park, IL (2003)

TRANSPORT ANALYSES OF 2–D CANDU DIFFUSION CALCULATIONS

G. Marleau and E. Varin
Institut de genie nucleaire, École Polytechnique de Montréal
C.P. 6079, succ. Centre-ville, Montréal, Québec H3C 3A7
guy.marleau@polymtl.ca; elisabeth.varin@polymtl.ca

ABSTRACT

We analyze using diffusion and transport theory methods an axially infinite 2–D representation of a CANDU reactor fueled with 37 element bundles. Our studies indicate that a relatively fine mesh is required to ensure that the reactor model is spatially converged for both diffusion and transport calculations. The use of the more physical cylindrical boundary condition in diffusion theory leads to a better simulation of the transport problem with an annular reflector description. The flux distribution computed using diffusion theory are more peaked towards the core center than their transport counterpart the differences being larger near the core/reflector interface. The Cartesian and annular transport model eigenvalues indicate that the diffusion theory model simulates relatively well the coolant void reactivity coefficient.

Key Words: CANDU reactor, transport and diffusion theory

1. INTRODUCTION

Most CANDU reactor simulations are performed using deterministic diffusion theory methods because it is believed that this approximation is generally adequate to represent the neutron behavior inside the core. 3–D Cartesian models are considered and codes such as RFSP [1], DONJON [2] or NESTLE [3] are used to evaluate the flux and power distribution inside the core based on burnup dependent two group fuel cell properties generated using the cell codes WIMS-AECL [4], DRAGON [5] or HELIOS [6].

The apparition of more powerful computers has made it possible to consider evaluating 3–D Monte-Carlo transport solutions for finite CANDU reactors [7, 8]. Such solutions are expensive and cannot be used for the day to day simulations required for CANDU fuel management studies. In addition, they are often performed on simplified models of the reactor core [7]. Nevertheless, the Monte-Carlo solutions can be used to quantify the errors resulting from the use of the diffusion approximation. Actually, using diffusion theory methods implies that the boundary conditions are approximated by zero flux conditions on an extrapolated boundary. The validity of Fick's law can also be questioned at the core reflector interface where large changes in physical properties are observed. These two approximations could lead to large flux differences in the reflector and in the last radial fuel regions, thereby affecting the precision of the computed bundle powers.

The main problem with the comparison of MCNP [9] based 3–D Monte-Carlo solutions and the standard deterministic diffusion calculations is the fact that they are generally performed using different cross section libraries. Most Monte-Carlo calculations are based on a continuous energy cross sections library while two-group cell average properties are used for the deterministic diffusion calculations. It is therefore difficult to identify in such comparisons the effect of cross section library differences from that resulting

from the use of the diffusion approximation. In order to be able to quantify the errors resulting from the use of the diffusion approximation it is therefore necessary to perform the diffusion and the reference transport calculations using identical cross section library. This can be achieved easily using the collision probability (CP) based transport code DRAGON and the diffusion code DONJON. The only constraint is to make sure that the transport and diffusion solutions are both spatially converged. Because the flat source assumption is the main approximation in CP based codes, a fine mesh discretization is required to ensure that a reliable transport solution is obtained. The amount of memory necessary to generate a converged CP transport solution for the full 3–D reactor is considerable which is why we considered an axially infinite 1/8 core 2–D model for the reactor.

The goal of this study is to establish a reactor transport solution that can be used as a reference against which diffusion solutions can be compared. Thus a simplified 2–D representation of the reactor is presented and studied in the context of deterministic diffusion and transport calculations. Comparison between the transport and diffusion fluxes distributions are used to quantify the errors that can be associated with diffusion theory. Both cooled and fully voided (coolant removed) representations of the core are considered.

2. MODELS

2.1. Cell Models

Before discussing in details the 2–D reactor models considered in this analysis, it is important to discuss first the generation of the cell properties required in our calculations. Here the reactor is fueled with the standard 37 element CANDU–6 bundles [8]. The burnup dependent cross sections are generated using the DRAGON code where one assumes that the fuel depletes at a fixed power density of 31.97 kW/kg during 300 days with time steps of 1 day.

At each time step, the DRAGON computed multi-group and multi-region flux distribution is used to obtain two-group homogenized cross sections that are stored in a fuel-burnup dependent reactor database. Two different cell homogenization options are considered, namely, a full cell homogenization and a 3 region homogenization where the properties of the fuel, the pressure to calandria tubes and the moderator are homogenized independently. For the latter case, the SPH homogenization procedure [10] is selected to ensure that a transport solution based on the 3 region properties results in the same eigenvalue and reaction rates as those obtained from the solution of the original multiregion transport problem.

2.2. Time-Average Models

The cell-average properties are then used for a 3–D reactor calculation in diffusion theory using the code DONJON. The goal of this calculation is to obtain a time-average burnup distribution in the core that can be used in our 2–D reactor model. A coarse mesh CANDU model without reactivity control devices is first selected. Two combustion zones are then defined and an average exit burnup is computed in such a way as to maintain a super-critical core with k_{eff}=1.020. This should account for the absence of the absorber rods (15 mk) and liquid zone controllers (5 mk) in our core model.

A channel age pattern is then considered to determine the specific burnup of each fuel bundle based on the resulting time-average burnup distribution [11]. To obtain a 2–D burnup distribution, the 4560 fuel bundle

burnups B_{ij} are averaged with respect to their respective powers P_{ij} using:

$$B_j = \sum_{i=1}^{12} B_{ij} P_{ij} / \sum_{i=1}^{12} P_{ij} \tag{1}$$

where j=1, 380 represents the bundle location in the $x-y$ plane and i=1, 12 indicates its location along the z-axis. The burnup distribution is transformed into a depletion time pattern, each time step being rounded of to an integer number of days. This rounding off is convenient because it avoids interpolation in the fuel tables (the cross sections tables are tabulated with time steps of 1 day). This procedure guarantees that the transport and diffusion calculations are performed using exactly the same two-group cross section library.

2.3. Diffusion Models

Our 1/8 core simplified CANDU 2–D model which is illustrated in Figure 1 simulates a mid-plane cut through a CANDU–6 at the location of maximal reflector thickness. It is defined on a Cartesian mesh in which virtual cells (empty boxes) represent the regions outside the annular calandria. Here, the reflector is redistributed inside selected Cartesian regions in such a way that the total reflector volume is preserved. The reflector region is divided into 5 meshes along the x and y axes, 4 of which are half a lattice pitch wide while the last mesh is 11.375 cm wide. Each fuel cell is also subdivided into 2 sub-regions in each direction x and y. This then yields a 27×27 region model. The properties of each fuel cell in the reactor depend on fuel burnup. The reflector properties are assumed burnup independent. Note that the CANDU reactor is not symmetric along the $x-y$ diagonal, and only 376 out of the 380 fuel channels are simulated in our 1/8 core model.

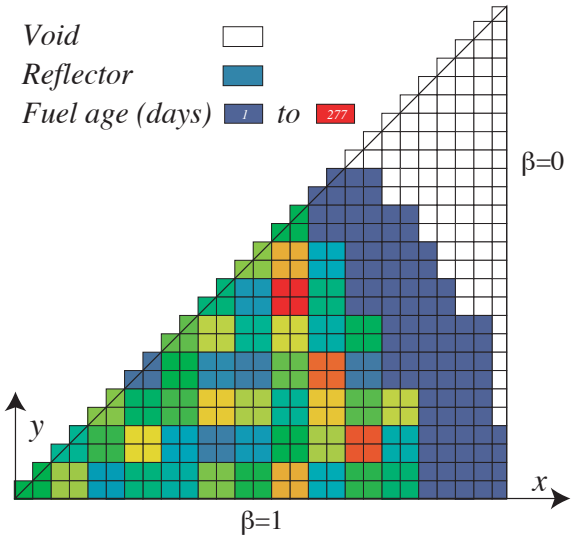

Figure 1. CANDU 1/8 core 2–D Cartesian model

Now, in order to obtain the neutron flux distribution inside the reactor, the boundary conditions used in diffusion theory must simulate as well as possible zero incoming flux conditions on the annular boundary associated with the limit of the calandria. In diffusion theory, this condition is approximated using: [12, 13]

$$\phi(\vec{r}_s) + 2D(\vec{r}_s)\vec{N}(\vec{r}_s) \cdot \vec{\nabla}\phi(\vec{r}_s) = 0 \tag{2}$$

where $\vec{N}(\vec{r}_s)$ is the outgoing unit normal on the external boundary. One can show that Eq. (2) is equivalent to a zero flux boundary condition at an extrapolated distance $\vec{r}_e = \vec{r} + \epsilon_r$.

This approximate boundary condition can be simulated in several ways inside the diffusion based reactor code DONJON. One can first assume that the flux vanishes at extrapolated distances $x + \epsilon_r$ and/or $y + \epsilon_r$ on the outer Cartesian surfaces associated with the reflector region. This approximation is called the *VOID* boundary condition. One can also use angle dependent Cartesian extrapolation distances $x + \epsilon_x(\theta)$ and $y + \epsilon_y(\theta)$ where $\epsilon_x(\theta)$ and $\epsilon_y(\theta)$ are first order approximations to ϵ_r [13]. This condition is called the cylindrical boundary condition.

2.4. Transport Models

Here three models are considered. The first model is similar to the 2–D CANDU Cartesian model used for the diffusion calculation (see Figure 1) with the virtual cells replaced by voided cells. As we observed before, this implies that the reflector present in the annular calandria is redistributed inside selected Cartesian regions. The zero re-entrant flux conditions are applied at the Cartesian limits of the reactor. This choice of boundary condition only approximates zero re-entrant flux at the reflector/void interface since some of the neutrons leaving the reflector region can re-enter the reflector after crossing the void region.

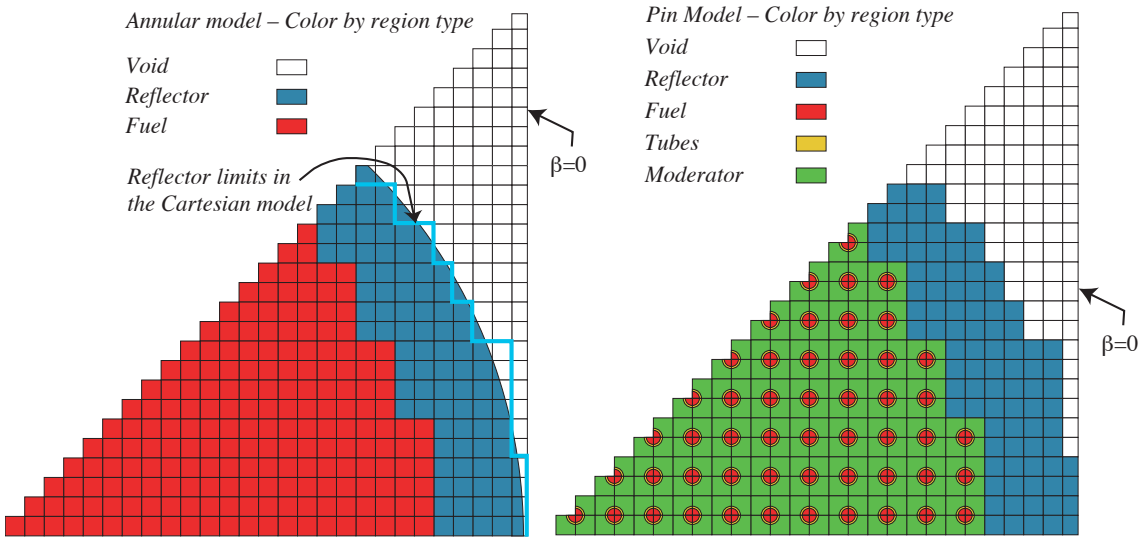

Figure 2. CANDU annular and pin models

For the second model, the annular reflector is modeled explicitly as illustrated in Figure 2. In this case, there is no need to redistribute the reflector inside selected Cartesian regions since each Cartesian region can be subdivided into a reflector and a voided region. Zero re-entrant flux conditions are again applied at the Cartesian limits of the reactor. However, in this case, the boundary conditions exactly simulate zero re-entrant flux at the reflector/void interface

Finally, the third model (pin model) is illustrated in Figure 2. Here the properties of each fuel cell in the reactor, which are homogenized over 3 regions depend again on fuel burnup. The reflector is again redistributed in selected Cartesian regions (similar to the Cartesian Model), and its properties remain

burnup independent. Using this model, one should be able to quantify the errors in the flux (and power) distribution inside the core due to the full cell homogenization.

3. DIFFUSION-DIFFUSION ANALYSES

3.1. Calculation Methodology

The diffusion equation is solved using the code DONJON. The mesh centered finite difference (MCFD) method implemented in the TRIVAC modules [14] is used for most of our analyses. However, for verification purposes, higher order finite difference methods were also studied [15]. In order to compare the results, fluxes are normalized in such a way that the total thermal power of the reactor is 2.0614 GW. To compare different mesh splitting, a flux homogenization is also realized on a coarse 14×14 region mesh, where each region is one lattice pitch wide except for the last x and y directed set of regions which are 11.375 cm wide.

3.2. Spatial Effects

We first considered the effect on the diffusion solution of refining the spatial mesh. The original 27×27 model with *VOID* boundary conditions is therefore subdivided into n=2, 3, 4 and 5 sub-regions in each direction x and y.

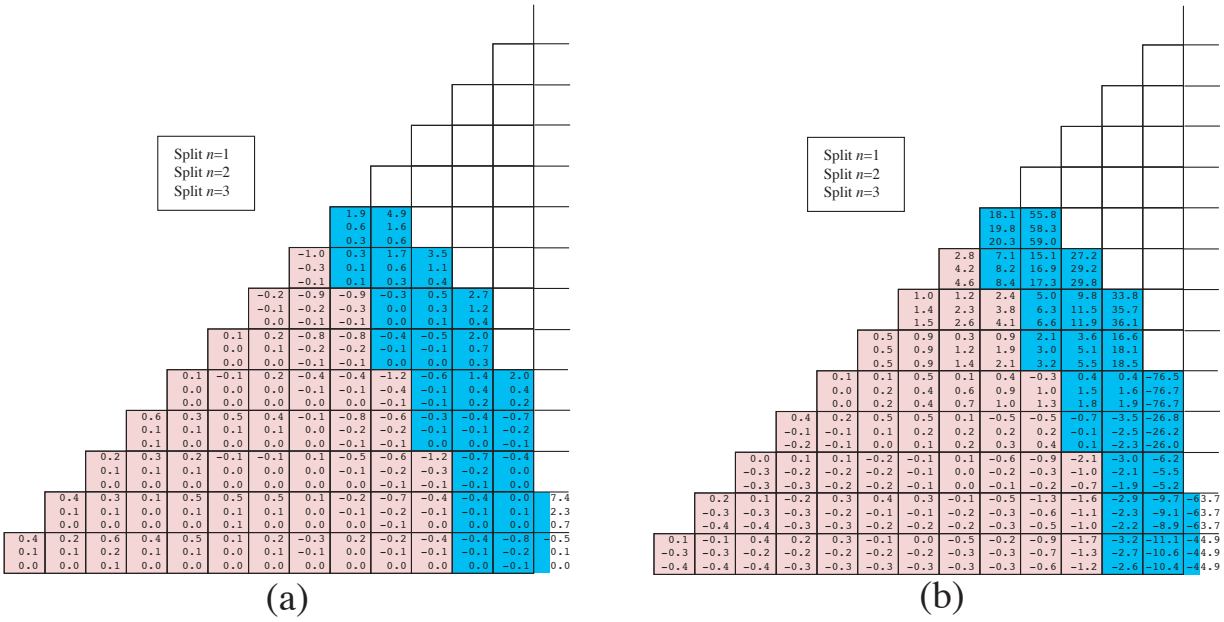

Figure 3. Relative differences in diffusion flux as a function of split level n (a) and effect of cylindrical boundary conditions on diffusion flux as a function of split level n (b)

The relative flux differences:

$$\Delta\phi = 100 \left(\frac{\phi - \phi^{\text{reference}}}{\phi^{\text{reference}}} \right) \tag{3}$$

between the coarse mesh solution (n=1, 2 and 3) and the reference very fine 135×135 mesh solution (n=5) are presented in Figure 3(a). As one can see, the flux is spatially converged to within 0.1 % in the fuel and to within 0.6 % in the reflector for a n=3 split in each direction.

We also compared, for various values of n, the results obtained using cylindrical and *VOID* (reference) boundary conditions (see Figure 3(b)). Here, one observes that the differences are nearly independent of the mesh splitting considered. The use of cylindrical boundary conditions leads to a decrease of 0.4 % in the flux at the centre of the core. This is compensated by an increase of up to 4.6 % in the flux for the fuel regions in contact with the reflector. Finally the flux in the reflector is, as expected, very strongly affected by the boundary conditions and the observed differences can be larger than 50 % in some regions. In fact, the very large differences ($>$ 50 %) arise in the Cartesian regions that were filled with reflector by the reflector redistribution process while they would contain a large amount of void if the exact annular geometry was considered (see Figure 2). The distances at which the interpolated flux is set to 0.0 in these cases are much shorter for the cylindrical than for the *VOID* BC which explains the large negative differences. From these comparisons one can conclude that the cylindrical boundary conditions contribute to a power increase in the outer ring of the reactor compared to *VOID* boundary conditions.

High order finite difference methods were also investigated. First (equivalent to mesh centered finite differences), second, third and fourth order nodal collocations were considered in the case of *VOID* boundary conditions (cylindrical boundary conditions are not implemented for high order finite difference methods). The differences observed are compatible to those obtained with our mesh splitting effort since the two approaches are comparable.

We repeated these analyses for the cases where the coolant in the pressure tube is removed. The results indicate that a mesh splitting of n=3 is also adequate for the voided configuration since the flux is also converged to within 0.1 % in the fuel region and to within 0.6 % in the reflector. The effect of changing the boundary conditions is also similar to that observed for the cooled case.

Even if all of these models show differences in fluxes distributions that can be considerable, their eigenvalues are very similar, even identical. Mesh splitting has almost no effect on eigenvalues either for cooled or voided cases ($<$ 0.04 mk differences in k_{eff}). For the model with *VOID* boundary conditions, the eigenvalue of the cooled reactor remains at k_{eff}=1.03294 while for the voided case it is k_{eff}=1.04778. Using cylindrical boundary conditions increases the eigenvalue by 0.06 mk for both coolant configurations. The coolant void reactivity, which is computed using

$$\rho = 1000 \left(\frac{k_{eff}^{\text{Voided}} - k_{eff}^{\text{Cooled}}}{k_{eff}^{\text{Voided}} k_{eff}^{\text{Cooled}}} \right) \tag{4}$$

is ρ=13.7 mk. This value, which is for a core containing only 376 fuel channels is, as expected, slightly smaller than the NESTLE computed value of 15.7 mk for a full 3–D reactor configuration [16].

4. TRANSPORT-TRANSPORT ANALYSES

4.1. Calculation Methodology

The transport equation is solved using the CP approach in the lattice code DRAGON. The main approximation that affects the precision of the results here is the requirement that the source must be flat inside each region of the calculation mesh considered. In general, this means that the mesh must be selected in such a way that it is smaller than the neutron mean free path inside each region. For our reactor model this implies a 2–D mesh size $<$1 cm^2 and consequently more than 600K individual regions in the model. The amount of memory that is required to execute DRAGON on such a large problem is $>$9 Tbytes. This is clearly out of reach for current computer systems. With our computers, the amount of memory available is around 1 Gbytes corresponding to a problem involving 7000 unknowns per group.

For our 2–D reactor model, the cross section variations from fuel region to fuel region are relatively weak and, in principle, a coarse mesh model can be selected. The main errors then arise because of the presence of the reflector and even more importantly of the void region. Near the reflector/void interface, one expects the neutron flux distribution in the reflector region to decrease rapidly as the distance from the center of the core increases. As a result the diffusion sources in the reflector are not flat. This should have a large effect on the flux distribution in the fuel cells located near this reflector. Accordingly, one should consider a fine radial mesh for the reflector zone as well as for the fuel region located near the reflector.

4.2. Spatial Effects

In order to study the spatial convergence of the transport solution, a series of calculations with different spatial meshes is performed. The 1/8 core model is subdivided into n = 2, 3 and 4 equal meshes in both the x and y directions resulting in an increase for the number of regions by factors of 4, 9 and 16 respectively. For the finer model (n=4) this lead to a 2–D mesh size of 3.57×3.57 cm^2 which can be compared with the original mesh (n=1) of 14.3×14.3 cm^2.

First, let us consider the Cartesian model and compare the reference solution provided when the finer mesh (n = 4) is used with the solution for n=1, 2 and 3. Using Eq. (3), one can then compute the relative error in the fluxes presented in Figure 4(a). As one can see, for n=3 the maximum difference in the flux inside the fuel zone is 1.3 %, while in the reflector this error can reach 7.3 %. The error in the flux for the void zone past the reflector is somewhat larger since it can reach 20 %. This means that for the simple Cartesian description of the reactor, one can expect uncertainties in the computed flux distribution in the fuel that are $<$1 % for the n=4 model. The transport flux in the reflector region could also be in error by up to 7 %. Finally, one should note that the use of a coarser spatial mesh leads to a flattening of the flux distribution inside the fuel region while in diffusion, the opposite effect is observed.

We also studied the effect of using an annular reflector boundary in the transport calculation. The mesh splitting that is selected for the reference Cartesian model and for the model with an annular reflector is n=4. The relative differences in the flux distribution homogenized over the 14×14 mesh are presented in Figure 4(b). One can observe that the effect of using an annular reflector on the flux distribution at the center of the core remains weak (differences $<$ 0.6 %) while the differences reach 4.6 % at the core/reflector interface and 48.2 % at the reflector/void interface.

The differences observed are mainly due to the redistribution of the reflector along the core boundary when

passing from the annular to the Cartesian model (see Figure 2). The large positive differences can be associated with the locations where the amount of reflector in the annular model is increased with respect to the Cartesian model and the large negative differences with the locations where the amount of reflector is decreased. In the Cartesian model, the effect of neutron crossing the void region before returning to the reflector does not seem to have a large impact on the flux distribution since the systematic positive differences expected from this approximation for cells located on the reflector/void interface are not observed.

One may also note by comparing the Cartesian and annular transport models that the differences observed in the flux distribution at the core/reflector interface (see Figure 4(b)) are very similar to the differences observed in diffusion when the *VOID* and cylindrical boundary conditions are compared (see Figure 3(b)). Finally, the fact that the annular model generates a finer mesh at the reflector/void interface than the Cartesian model could also account for a small part of the differences observed.

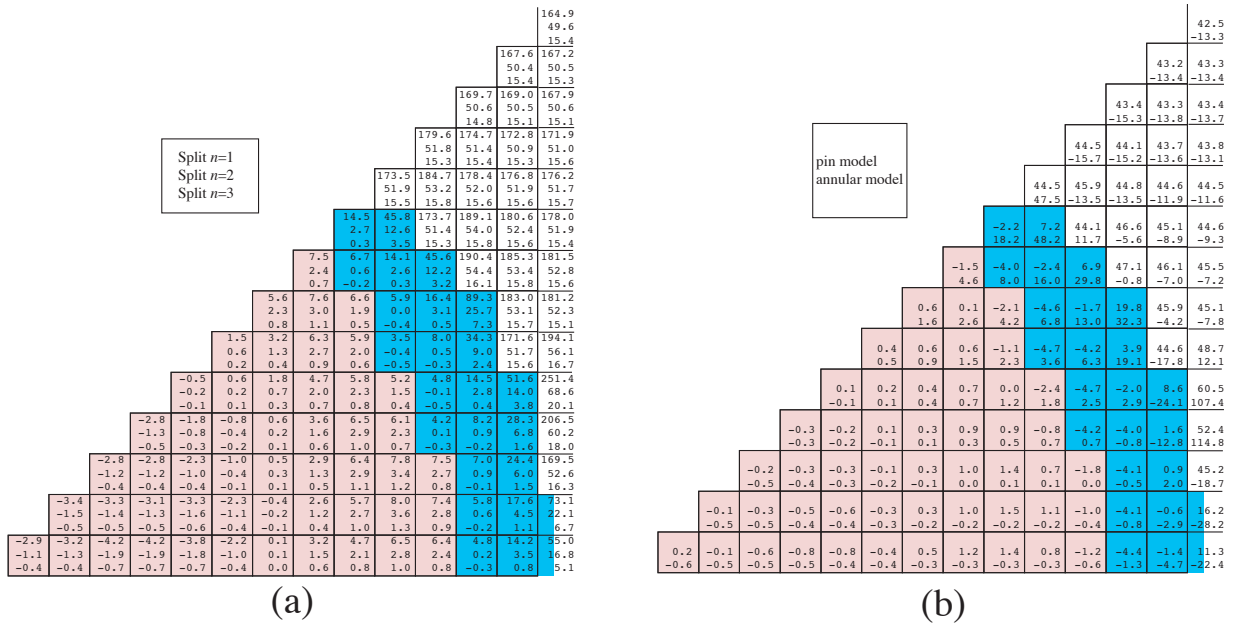

Figure 4. Relative differences in transport flux as a function of split level n (a) and effect of annularizing the reflector and pin description on transport flux (b)

For the comparison of the Cartesian and pin model, two different mesh splitting were chosen. For the reference Cartesian model we have selected the case where n=4. For the pin model, we use n=2 because of computer memory limitations. The relative differences in the flux distribution presented in Figure 4(b) indicates that the pin and Cartesian models converge to the same answer. Because of the fact that the pin model is inherently fine mesh in the cells containing the fuel pins, a n=2 mesh discretization in this case yields flux solutions in the fuel regions that are nearly equivalent to those obtained using a n=3 Cartesian solution. However, for the reflector and void regions, the differences are of the same order of magnitude as those observed for the n=2 Cartesian model.

We repeated all these transport calculations for the case where the coolant inside the pressure tube is removed. As we observed for the diffusion analysis, the general behavior of the transport solution as a

function of mesh splitting, boundary types or fuel model is identical to that observed for the cooled fuel calculations.

Table I. Eigenvalue and coolant void reactivity for various transport models

	Cartesian Model			Annular Model			Pin Model		
n	Cooled	Voided	ρ	Cooled	Voided	ρ	Cooled	Voided	ρ
1	1.002094	1.017456	15.1	1.002935	1.018292	15.0	1.001501	1.016956	15.2
2	1.022334	1.037567	14.4	1.022629	1.037862	14.4	1.013413	1.029107	15.0
3	1.029166	1.044373	14.1						
4	1.030703	1.045802	14.0	1.030982	1.046087	14.0			

Now let us look at the transport eigenvalues presented in Table I. Contrarily to the diffusion calculations the dependence of k_{eff} on mesh splitting is very important. For the Cartesian model, a change in eigenvalue of 28.6 mk is observed when refining the mesh from n=1 to 4. The rate of convergence of k_{eff} as a function of n is very rapid and the error $\Delta k_{\mathit{eff}}(n)$ can be approximated by:

$$\Delta k_{\mathit{eff}}(n) \approx 40e^{-\frac{n^2}{3}}$$

which means that the $n = 4$ results should be in error by about 0.2 mk.

The results for the Cartesian and annular models are similar for a specific value of n. This indicates that even if the type of boundary has a relatively large effect on the flux distribution in the core, the final effect on k_{eff} and ρ remains weak. On the other hand, the use of a pin instead of a homogeneous fuel model has a large impact on both k_{eff} and ρ. As a result, homogenizing the moderator with the fuel and coolant region increases substantially the eigenvalue leading to an overall decrease of the coolant void reactivity. Finally note that the void reactivity coefficient predicted using the diffusion model is 0.3 mk smaller than that obtained using the converged annular transport model. The difference in ρ is much larger for the n=2 pin model. However, the trend observed previously for the Cartesian and annular models suggests that this difference should decrease for a converged pin model.

5. TRANSPORT-DIFFUSION COMPARISON

We compared the n=3 diffusion models with *VOID* and cylindrical boundary conditions and our reference n=4 transport model with annular boundaries. The cooled and voided configurations are considered. The results we obtained are presented in Figure 5 where one can observe that both the cooled and voided configurations are equally well simulated using diffusion theory.

For the cooled and voided cases, the diffusion calculations lead to a 2 % over-estimation of the fluxes in the central core region with respect to the transport based calculations. Because the flux are normalized in such a way that all the models generate the same power, this automatically leads to an under-estimation that can reach 4 % for the fluxes in the outer fuel cells. These differences can be considered to be significant since

one expects from the analysis of Section 4.2 that the maximum error in the transport flux is smaller than 1 % in the fuel region. The diffusion flux in the reflector is also under-estimated with respect to the transport fluxes, the differences observed being much larger than the 7 % error associated with the transport solution in this region.

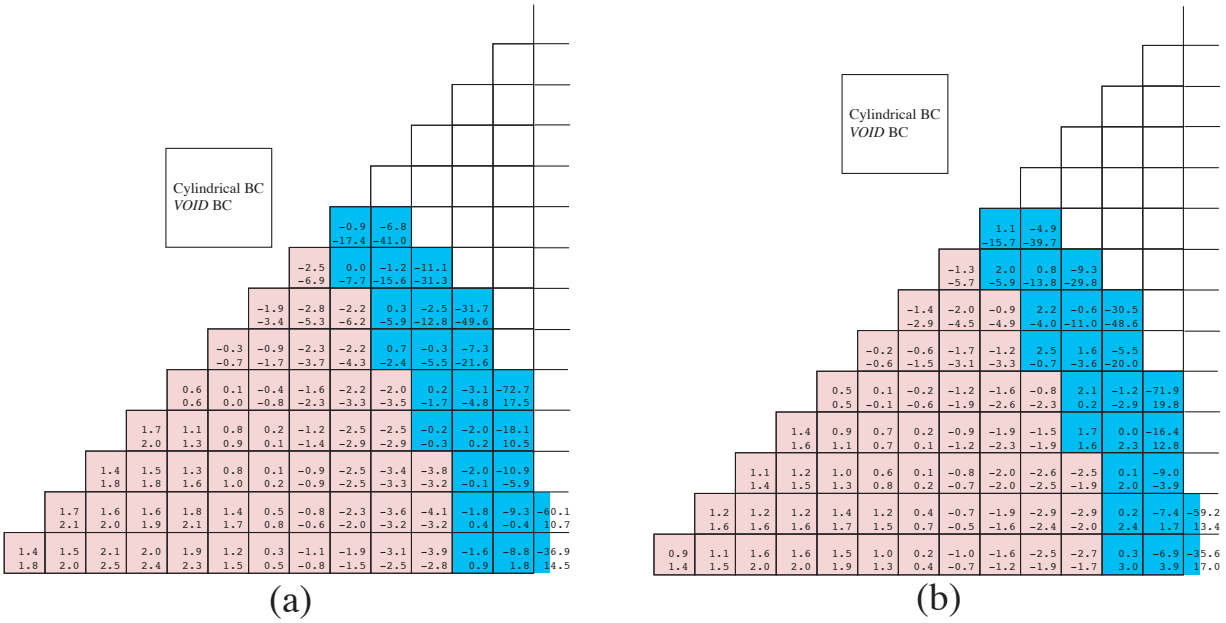

Figure 5. Difference between transport and diffusion fluxes for cooled (a) and voided (b) configurations

In general, the *VOID* boundary conditions yield larger errors in the diffusion flux for the fuel regions than cylindrical boundary conditions. In fact, a systematic reduction of nearly 0.3 % in the flux differences at the core center can be observed when using the more precise cylindrical boundary conditions. For the flux in the fuel regions in contact with the reflector, one can observe that the cylindrical boundary conditions while generating errors reaching 4.1 % again remain closer to the transport solution than the *VOID* boundary conditions which results in errors as high as 6.9 %. The same behavior is also observed for the reflector fluxes, except at the reflector/void interface where both boundary conditions lead to very large errors.

6. CONCLUSIONS

A simplified 2–D model for the CANDU reactor has been analyzed using transport and diffusion theory methods. This model was used to evaluate the errors in the flux distribution at the core/reflector interface resulting from the use of the diffusion approximation. The effect of using various approximations for the boundary conditions in both the transport and the diffusion models was also investigated. Finally, we studied how the use of a pin model for each cell in the reactor would change the flux distribution in the core compared to the flux distribution obtained using the standard homogeneous cell model.

In order to ensure that the diffusion and the transport solutions are converged a relatively fine spatial calculation mesh is required. In diffusion we observed differences in the fuel and reflector flux distribution

that remain smaller than 0.1 % and 1.0 % respectively only for the case where the mesh size is < 25 cm^2. In transport, the requirements for spatial convergence are even more stringent and errors in the flux distribution of 1.3 and 7.3 %, for the fuel and reflector regions respectively, were observed with the finest mesh (≈ 16 cm^2) we could achieve (Cartesian and annular models). For the pin model, spatial convergence was not fully achieved, but our results indicate that the flux distribution in the fuel region is coherent with that obtained using our fine mesh Cartesian model. Even if the size of the mesh has a large effect on the flux distribution when the diffusion model is considered, its effect on k_{eff} or on the coolant void reactivity remains very small. If fact, the maximum difference in the diffusion eigenvalue observed between the coarser and finer mesh is 0.04 mk. In transport, both the eigenvalue and the coolant void reactivity are very sensitive to the spatial discretization and the extrapolated error in k_{eff} for our finest mesh is still around 0.2 mk. Finally, the $n = 4$ transport theory model with an annular representation of the reflector boundary is currently the best model that can be simulated using the CP method in the code DRAGON.

Our results indicate that the flux distribution in the outer fuel rings is under estimated by up to 4 % in diffusion theory. The diffusion flux in the reflector is also smaller than the transport flux. As expected, the transport theory flux solutions obtained using the annular model is better simulated when cylindrical rather than *VOID* boundary conditions are used in diffusion theory.

ACKNOWLEDGMENTS

This work was supported in part by a grant from the Natural Sciences and Engineering Research Council of Canada and by the Hydro-Québec chair in Nuclear Engineering.

REFERENCES

[1] B. Rouben, *An overview of Current RFSP-Code Capabilities for CANDU Core Analysis*, Atomic Energy of Canada Limited, Report AECL-11407 (1996).

[2] E. Varin, A. Hébert, R. Roy and J. Koclas, *A Users Guide for DONJON*, Report IGE-208, Institut de Génie Nucléaire, École Polytechnique de Montréal (2000).

[3] P.J. Turinsky, R.M.K. Al-Chalabi, P. Engrand, H.N. Sarsour, F.X. Faure and W. Guo, *NESTLE: A Few-Group Neutron Diffusion Solver Utilizing the Nodal Expansion Method for Eigenvalue, Adjoint, Fixed-Source Steady-State and Transient Problems*, EGG-NRE-11406, Idaho National Engineering Laboratory (1994).

[4] J.V. Donnelly, *WIMS-CRNL: A Users Manual for the Chalk River Version of WIMS*, Atomic Energy of Canada Limited, Report AECL-8955 (1986).

[5] G. Marleau, A. Hébert and R. Roy, *A Users Guide for DRAGON*, Report IGE-174 Rev. 5, Institut de Génie Nucléaire, École Polytechnique de Montréal (2000).

[6] J.J. Casal, R.J.J Stammler, E.A. Villarino and A.A. Ferri, "HELIOS: Geometric Capabilities of a New Fuel-Assembly Program," *Intl. Topical Meeting on Advances in Mathematics, Computations, and Reactor Physics*, Pittsburgh, Pennsylvania, April 28-May 2, 1991.

[7] F. Rahnema, S. Mosher, M. Pitts, P. Akhtar and D. Serghiuta, "MCNP Simulation of Void Reactivity in a Simplified CANDU Core Sub-Region", *Monte-Carlo-2000*, Lisbon, 2000.

[8] K.S. Kozier, "Assessment of CANDU Reactor Physics Effects Using a Simplified Whole-Core MCNP Model", *PHYSOR 2002*, Seoul Korea, October 7-10, 2002 A Transport Analysis of 2–D CANDU

[9] J.F. Briesmeister (editor), *MCNP – A General Monte Carlo N-Particle Transport Code, Version 4B*, Los Alamos National Laboratory Report, LA-12625-M, Version 4B, UC 705 and UC 700 (1997).

[10] A. Hébert, "Development of a Second Generation SPH Technique for the Pin-by-Pin Homogenization of a Pressurized Water Reactor Assembly in Hexagonal Geometry", *Trans. Am. Nucl. Soc.*, **71**, 253 (1994).

[11] D. Rozon and W. Shen, "A Parametric Study of the DUPIC Fuel Cycle to Reflect Pressurized Water Reactor Fuel Management Strategy", *Nucl. Sci. Eng.*, **138**, 1-25 (2001).

[12] F. Rahnema and G.C. Pomraning, "On Linear Extrapolation Distances. Extrapolated Endpoints, and Eigenvalues", *Nucl. Sci. Eng.*, **77**, 438-443, (1981).

[13] R. Roy, D. Rozon, A. Hébert and G. Hotte, "Treatment of Circular Boundary Conditions in Neutron Diffusion Calculations", *Third International Conference on Simulation Methods in Nuclear Engineering*, Montréal, Québec, April 18-20, 1990.

[14] A. Hébert, "TRIVAC, A Modular Diffusion Code for Fuel Management and Design Applications", *Nucl. J. of Canada*, **1**, 325 (1987).

[15] A. Hébert, "Development of the Nodal Collocation Method for Solving the Neutron Diffusion Equation", *Ann. Nucl. Energy*, **14**, 527-541 (1987).

[16] H.N. Sarsour, F. Rahnema, S. Mosher, P.J. Turinsky, D. Serghiuta, G. Marleau and T. Courau, "HELIOS/DRAGON/NESTLE Codes Simulation of Void Reactivity in a CANDU Core", *CNS Twenty-Second Nuclear Simulation Symposium*, Ottawa, Ontario, November 3-5, 2002.